Optimal periodic resource allocation in reactive dynamical systems: Application to microalgal production

Olivier Bernard, Liu-Di Lu, Julien Salomon

Optimization of mixing strategy in microalgal raceway ponds

Olivier Bernard[1], Liu-Di LU[1,2], Julien Salomon[2]

[1] *Université Nice Côte d'Azur, Inria BIOCORE, BP93, 06902 Sophia-Antipolis Cedex, France*

[2] *Inria ANGE, 75589 Paris Cedex 12, France and Sorbonne Université, CNRS, Laboratoire Jacques-Louis Lions, 75005 Paris, France*

Abstract

This paper focuses on mixing strategies to enhance the growth rate in an algal raceway system. A mixing device, such as a paddle wheel, is considered to control the rearrangement of the depth of the algae cultures hence the light perceived at each lap. The dynamics of the photosystems after a rearrangement is accounted for by the Han model. Our approach consists in considering permanent regimes where the strategy is parametrized by a permutation matrix which modifies the order of the layers at the beginning of each lap. It is proven that the dynamics of the photosystems is then periodic, with a period corresponding to one lap of the raceway whatever the order of the considered permutation matrix is. An objective function related to the average growth rate over one lap is then introduced. Since $N!$ permutations (N being the number of considered layers) need to be tested in the general case, it can be numerically solved only for a limited number of layers. Consequently, we propose a second optimization problem associated with a suboptimal solution of the initial problem, which can be determined explicitly. A sufficient condition to characterize cases where the two problems have the same solution is given. Some numerical experiments are performed to assess the benefit of optimal strategies in various settings.

1 Introduction

Microalgae are photosynthetic microorganisms whose potential has been highlighted in the last decade, especially for feed, food, renewable energy and wastewater treatment [26, 19, 24]. In comparison with terrestrial plants, whose growth is reduced due to the CO_2 availability, the high actual photosynthetic yield of microalgae cultures leads to large algal biomass productions potential. Meanwhile, they also have a great potential on numerous high added value commercial applications: pharmaceutical, cosmetics or pigments [15, 25]. Depending on the

source of the light, these microorganisms are generally cultivated at industrial scale in open or closed photobioreactors. These devices vary from the most simple and cheap open raceway ponds to some high-tech photobioreactors. In this paper, we limit ourselves to the industrial production of microalgae in a raceway pond.

A standard raceway pond is a circular basin where the algae are exposed to solar radiation. This hydrodynamic system is set in motion by a paddle wheel which homogenises the medium for ensuring an equidistribution of the nutrients and guarantees that each cell will have regularly access to the light [9]. The algae in the system are periodically harvested, and their concentration is maintained around an optimal value [23]. Different strategies have been proposed to maximize the production of the biomass in this algal raceway system [13, 12, 11, 10, 1]. For instance, theoretical works have determined the optimal biomass for maximizing the productivity [17, 2]. In [3], non flat topographies of the raceway bottom have been observed to improve slightly the growth rate of the algae in specific cases, e.g. when an extra mixing strategy is considered [4, 5].

In the current study, we use the Han dynamics to model the algae growth in a flat raceway system with a constant average velocity. We analyze in detail the previous mixing strategy together with its approximation by an explicitly solvable problem. More precisely, extending the study of [6], we give a specific criterion to check that the original problem and its approximation have the same solution. We also present some tests to show the efficiency of the mixing strategies and its approximation. Note that in the examples considered in our numerical tests, such mixing strategies give rise to significant improvements of the biomass production.

The paper is organised as follows. In Section 2, we present the models associated with the biological and the mixing device. This allows us to get explicit formula to determine the growth of microalgae during the production process. We then introduce the optimization problem and an approximation whose solution is explicit. A specific criterion to evaluate the approximation efficiency is given in Section 3. We then illustrate the performance of our strategies by numerical experiments in Section 4.

Notation. In what follows, $\mathbb{N}$ denotes the set of non-negative integers, $\mathcal{P}_N$ denotes the set of permutation matrices of size $N \times N$ with $N \in \mathbb{N}$ and $\mathfrak{S}_N$ denotes the associated set of permutations of N elements. The cardinal of a set E is denoted by $\#E$. Given a matrix M, we denote by $\ker(M)$ its kernel and by $M_{i,j}$ its coefficient (i, j). In the same way, W_n denotes the n-th coefficient of a vector W.

2 Raceway modeling and optimization

In this section, we present a model that describes the growth of the algae when traveling along the raceway and formulate the associated optimization problem.

2.1 Han model

We consider the Han model [18] to describe the dynamics of the photosynthetic units. In this compartmental model, each unit is assumed to have three different states: open and ready to harvest a photon (A), closed while processing the absorbed photon energy (B), or inhibited if several photons have been absorbed simultaneously leading to an excess of energy (C). Their dynamics is described by the following system

$$\begin{cases} \dot{A} = -\sigma_H I A + \dfrac{1}{\tau} B, \\ \dot{B} = \sigma_H I A - \dfrac{1}{\tau} B + k_r C - k_d \sigma_H I B, \\ \dot{C} = -k_r C + k_d \sigma_H I B. \end{cases}$$

Here A, B and C are the relative frequencies of the three possible states with $A+B+C = 1$, and I is a continuous time-varying signal representing the photon flux density. The coefficient σ_H stands for the specific photon absorption, τ is the turnover rate, k_r represents the photosystem repair rate and k_d is the damage rate. As shown in [21], one can use a fast-slow approximation and singular perturbation theory to reduce this system to a single evolution equation on the photo-inhibition state C:

$$\dot{C} = -\alpha(I)C + \beta(I), \tag{1}$$

where

$$\alpha(I) := k_d \tau \frac{(\sigma_H I)^2}{\tau \sigma_H I + 1} + k_r, \quad \beta(I) := k_d \tau \frac{(\sigma_H I)^2}{\tau \sigma_H I + 1}.$$

The net specific growth rate is obtained by balancing photosynthesis and respiration, which gives

$$\mu(C, I) := -\gamma(I)C + \zeta(I), \tag{2}$$

where

$$\gamma(I) := \frac{k_H \sigma_H I}{\tau \sigma_H I + 1}, \quad \zeta(I) := \frac{k_H \sigma_H I}{\tau \sigma_H I + 1} - R.$$

Here, R denotes the respiration rate and k_H is a factor which relates the photosynthetic activity to the growth rate.

We assume that the photosynthetic units grow slowly, so that the biomass variations are negligible over one lap of the raceway. In such a time scale, the turbidity is supposed to be constant and the Beer-Lambert law can be used to describe the light attenuation as a function of the depth z, i.e.

$$I(z) = I_s \exp(\varepsilon z), \tag{3}$$

where I_s is the light intensity at the free surface and ε is the light extinction coefficient. We assume that the system is perfectly mixed so that the concentration of the biomass is homogeneous, meaning that ε is constant. The average net specific growth rate over the domain is then defined by

$$\bar{\mu} := \frac{1}{T} \int_0^T \frac{1}{h} \int_{-h}^0 \mu\big(C(t,z), I(z)\big) \mathrm{d}z \mathrm{d}t, \tag{4}$$

where h is the depth of the raceway pond and T is the average duration of one lap of the raceway pond.

In order to compute numerically (4), we introduce a vertical discretization of the fluid. More precisely, we consider N layers uniformly distributed on a vertical grid. The depth of the layer n is given by

$$z_n := -\frac{n-\frac{1}{2}}{N}h, \quad n = 1, \dots, N. \tag{5}$$

For a given initial photo-inhibition state $C_n(0)$, let $C_n(t)$ be the solution of (1) at time t. In this semi-discrete setting, the average net specific growth rate in the raceway pond can be defined by

$$\bar{\mu}_N := \frac{1}{T}\int_0^T \frac{1}{N}\sum_{n=1}^{N} \mu(C_n(t), I_n)\mathrm{d}t, \tag{6}$$

where I_n is the light intensity received in the layer n.

2.2 Mixing device modeling

The mixing process is modelled by a permutation matrix $P \in \mathcal{P}_N$ as follows. Denote by $\sigma \in \mathfrak{S}_N$ the permutation corresponding to P. At each lap, the algae in the layer n are supposed to be entirely transferred into the layer $\sigma(n)$ when passing through the mixing device. This model is depicted schematically on an example in Figure 1.

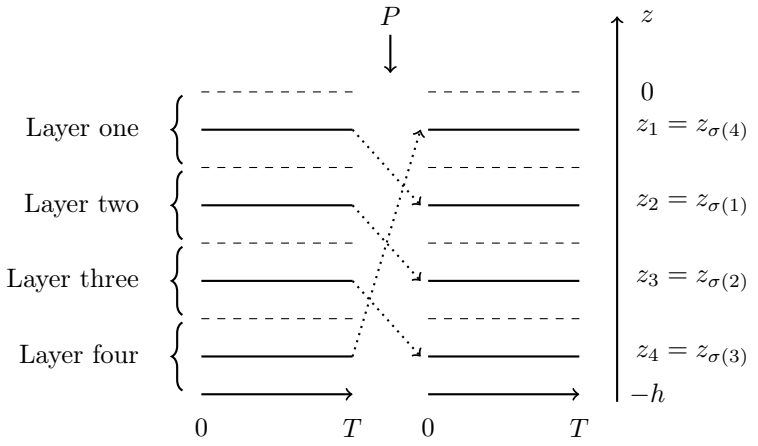

Figure 1: Schematic representation of the mixing process over two laps. Here, $N = 4$ and P corresponds to the cyclic permutation $\sigma = (1\ 2\ 3\ 4)$.

The interest of such a device is to mix the algae to better balance their exposure to light and increase the production. Note that in actual raceway ponds, this device is generally a paddle wheel (see for example [14]).

2.3 Explicit computation of the growth rate

Since $(I_n)_{n=1}^N$ are constant with respect to time, the solution of (1) can be computed explicitly. Indeed, for a given initial vector of states $(C_n(0))_{n=1}^N$, we have

$$C(t) = D(t)C(0) + V(t), \quad t \in [0, T], \tag{7}$$

where $D(t)$ is a time dependent diagonal matrix with $D_{nn}(t) := e^{-\alpha(I_n)t}$ and $V(t)$ is a time dependent vector with

$$V_n(t) := \frac{\beta(I_n)}{\alpha(I_n)}(1 - e^{-\alpha(I_n)t}). \tag{8}$$

It follows that (6) satisfies

$$\bar{\mu}_N = \frac{1}{NT}\Big(\langle \Gamma, C(0)\rangle + \langle \mathbf{1}, Z\rangle\Big), \tag{9}$$

where $\mathbf{1}$ is a vector of size N whose coefficients are equal to 1, and Γ, Z are two vectors such that

$$\Gamma_n := \frac{\gamma(I_n)}{\alpha(I_n)}(e^{-\alpha(I_n)T} - 1),$$
$$Z_n := \frac{\gamma(I_n)\beta(I_n)}{\alpha(I_n)^2}(1 - e^{-\alpha(I_n)T}) - \frac{\gamma(I_n)\beta(I_n)}{\alpha(I_n)}T + \zeta(I_n)T.$$

More details about the computations giving rise to (7) and (9) are presented in Appendix A.

2.4 Periodic regime

In this section, we study the evolution over multiple laps. For the sake of simplicity, we write hereafter D, V instead of $D(T), V(T)$. Recall that P is the permutation matrix associated with the considered mixing device. We denote by $C^k(0)$ the photo-inhibition state of the algae which has just passed the mixing device after k laps. According to (7) and by definition of P, we have

$$C^{k+1}(0) = P(DC^k(0) + V).$$

Before studying the sequence $\big(C^k(0)\big)_{k\in\mathbb{N}}$, let us give a technical result. We denote by $\mathcal{I}_N$ the identity matrix of size N.

Lemma 1. *Given $k \in \mathbb{N}$ and $P \in \mathcal{P}_N$, the matrix $\mathcal{I}_N - (PD)^k$ is invertible.*

Proof. Assume $\mathcal{I}_N - PD$ is not invertible, then there exists a non-null vector $X \in \ker(\mathcal{I}_N - PD)$, which means $X = PDX$. Let us denote $d_n = D_{nn}$, $n = 1, \dots, N$. Denoting by σ the permutation associated with P, we find that $(DX)_n = d_n X_n$ and $X_n = (PDX)_n = d_{\sigma(n)} X_{\sigma(n)}$. In the same way, we have

$X_n = \big((PD)^k X\big)_n = d_{\sigma^k(n)} \dots d_{\sigma(n)} X_{\sigma^k(n)}$, where $\sigma^k(n)$ denotes the $k-$times repeated composition of σ with itself. Denoting by K the order of σ, we have

$$X_n = \big((PD)^K X\big)_n = d_{\sigma^K(n)} \cdots d_{\sigma(n)} X_{\sigma^K(n)} = d_{\sigma^K(n)} \cdots d_{\sigma(n)} X_n.$$

Since, $0 < d_n < 1$ for $n = 1, \dots, N$, then $0 < d_{\sigma^K(n)} \cdots d_{\sigma(n)} < 1$. This implies that $X_n = 0$, which contradicts our assumption. Therefore, $\mathcal{I}_N - PD$ is invertible. That $\mathcal{I}_N - (PD)^k$ is invertible can be proved in much the same way. □

Assume now that the state C is KT-periodic in the sense that after K times of passing the device P, we have $C^K(0) = C(0)$. A crucial property of $\big(C^k(0)\big)_{k\in\mathbb{N}}$ is given in the next proposition.

Proposition 1. *We keep the notation of the previous lemma. For all $k \in \mathbb{N}$, we have*

$$C^k(0) = (\mathcal{I}_N - PD)^{-1} PV.$$

As a consequence, the sequence $\big(C^k(0)\big)_{k\in\mathbb{N}}$ is constant.

Proof. Thanks to Lemma 1, there exists a unique $\bar{C}$ satisfying $\bar{C} = P(D\bar{C} + V)$. Let us then define the sequence $(e^k)_{k\in\mathbb{N}}$ by $e^k := C^k(0) - \bar{C}$. We have $e^{k+1} = (PD)e^k$. Since C is assumed to be KT-periodic, we have $e^0 = e^K = (PD)^K e^0$. According to Lemma 1, $\mathcal{I}_N - (PD)^K$ is invertible, meaning that $e^0 = 0$. It follows that $e^k = 0$, for $k \in \mathbb{N}$. The result follows. □

A natural choice for K would be the order of the permutation associated with P. Indeed, in this case K is the minimal number of laps required to recover the initial ordering of the layers. The previous result shows that every $KT-$periodic evolution will actually be $T-$periodic. In the next section, we show that this property is decisive to formulate an optimization problem associated with $\bar{\mu}_N$. In addition, the computations to solve the optimization problem will be reduced, since the CPU time required to assess the quality of a permutation will not depend on its order.

2.5 Optimization of the growth rate

Recall that the light intensity I is assumed to be constant with respect to time. As a consequence, Γ and Z have the same value at each lap. With the help of (9), the average net specific growth rate for K laps of the raceway pond is then defined by

$$\bar{\mu}_N^K := \frac{1}{K} \sum_{k=0}^{K-1} \bar{\mu}_N^k = \frac{1}{K} \sum_{k=0}^{K-1} \frac{1}{NT} \Big(\langle \Gamma, C^k(0) \rangle + \langle \mathbf{1}, Z \rangle \Big).$$

Assuming the system to be KT-periodic, we get from Proposition 1 that $\bar{\mu}_N^K = \bar{\mu}_N$, meaning that we only need to consider the evolution over one lap of raceway. Replacing now $C(0)$ in (9) by (1), we obtain

$$\bar{\mu}_N = \frac{1}{NT} \Big(\langle \Gamma, (\mathcal{I}_N - PD)^{-1} PV \rangle + \langle \mathbf{1}, Z \rangle \Big). \tag{10}$$

Since N, T and Z do not depend on P, we focus on the objective function defined by

$$J_H(P) := \langle \Gamma, (\mathcal{I}_N - PD)^{-1} PV \rangle. \tag{11}$$

The optimization problem then reads:

Find a permutation matrix $P_{\max}$ solving the maximization problem:

$$\max_{P \in \mathcal{P}_N} J_H(P). \tag{12}$$

2.6 Approximation of the optimization problem

Since $\#\mathfrak{S}_N = N!$, Problem (12) cannot be tackled in realistic cases where large values of N must be considered, e.g., to keep a good numerical accuracy. To overcome this difficulty, we propose in this section an approximation of (11) whose optimum can be determined explicitly. For this purpose, we expand the functional (11) as follows

$$\langle \Gamma, (\mathcal{I}_N - PD)^{-1} PV \rangle = \sum_{l=0}^{+\infty} \langle \Gamma, (PD)^l PV \rangle = \langle \Gamma, PV \rangle + \sum_{l=1}^{+\infty} \langle \Gamma, (PD)^l PV \rangle,$$

and consider as an approximation the first term of this series, namely

$$J_H^{\text{approx}}(P) := \langle \Gamma, PV \rangle. \tag{13}$$

The associated optimization problem then reads:

Find a permutation matrix P_+ solving the maximization problem:

$$\max_{P \in \mathcal{P}_N} J_H^{\text{approx}}(P). \tag{14}$$

In the following, we prove that when a specific criterion is satisfied, Problem (14) and Problem (12) have the same solution. In this case, the optimal strategy can be determined explicitly once the vectors Γ and V are given.

3 General optimization problem

In this section, we consider an abstract formulation of the previous problems and present a criterion to compare their solutions.

3.1 Abstract formulation

Let $u, v \in \mathbb{R}^N$ two arbitrary vectors. We now consider both minimization and maximization problems associated with the functional

$$J(P) := \langle u, (\mathcal{I}_N - PD)^{-1} Pv \rangle, \tag{15}$$

where $P \in \mathcal{P}_N$ Here, we keep the notation D, even though it is now considered in a more generic way, namely a diagonal matrix with entries belonging to $[0, 1)$.

This setting includes the optimization problem associated with the algal raceway model introduced in the previous sections. Indeed, u and v stand for Γ and V, respectively, whereas the objective function J corresponds to J_H defined in (11). Its approximation is then defined by

$$J^{\text{approx}}(P) := \langle u, Pv \rangle. \tag{16}$$

Without loss of generality (see Appendix B for the details), we assume that the entries of u are sorted in an ascending order, meaning that $u_1 \leq \ldots \leq u_N$. Note that optimizing J^{approx} amount to solving an assignment problem [8]. Indeed, we have for example

$$\min_{P \in \mathcal{P}_N} J^{\text{approx}}(P) = \min_{\sigma \in \mathfrak{S}_N} \sum_{n=1}^{N} u_n v_{\sigma(n)}.$$

This problem reads as a linear assignment problem associated with the matrix $[u_i v_j]_{(i=1,\ldots,N\ ;\ j=1,\ldots,N)}$. To make our exposition self-contained, we give the solution of this problem in Section 3.3.

Remark 1. *A fairly common approach to deal with permutation optimization is to relax the problem by extending the optimization to the set of bistochastic matrices. As an example, this technique corresponds to the Kantorovitch relaxation considered in optimal transport [20], see also [7] for a more general presentation of the linear case, and [22] for a similar strategy in the context of quantum chemistry. This approach allows the optimization to be performed by gradient-type methods. At the theoretical level, the goal is then to prove that the convergence takes place towards extremal points, i.e. permutation matrices. We have tested this approach to the nonlinear problem* (15)*. Our results indicate that the obtained limits are indeed permutation matrices. However, we observed that the obtained matrices are not always optimal, which leads us to conjecture the existence of local non-global minima for this extended form of J.*

3.2 Some technical lemmas

Let us state some preliminary properties about the permutation set $\mathfrak{S}_N$ that we will use in the next section. Given $k \in \mathbb{N}$, and two arbitrary permutations $\sigma, \widetilde{\sigma} \in \mathfrak{S}_N$, let us define

$$\begin{aligned} E_k(\sigma, \widetilde{\sigma}) &:= \left\{ n = 1, \ldots, N \mid \sigma^k(n) \neq \widetilde{\sigma}^k(n) \right\}, \\ G_k(\sigma, \widetilde{\sigma}) &:= \{ n = 1, \ldots, N \mid \forall k' \leq k,\ \sigma^{k'}(n) = \widetilde{\sigma}^{k'}(n) \}, \end{aligned}$$

and $m_k := \# E_k(\sigma, \widetilde{\sigma})$. We have the following result.

Lemma 2. *For $k \in \mathbb{N}$, we have $m_k \leq k m_1$ and $\# G_k(\sigma, \widetilde{\sigma}) \geq \max(N - k m_1, 0)$.*

Proof. To shorten notation, we write in this proof E_k instead of $E_k(\sigma, \widetilde{\sigma})$, E_{k+1} instead of $E_{k+1}(\sigma, \widetilde{\sigma})$, G_k instead of $G_k(\sigma, \widetilde{\sigma})$, etc. From the definition of E_k, we have:

$$E_{k+1} = ((\{1, \ldots, N\} \setminus E_1) \cap E_{k+1}) \cup (E_1 \cap E_{k+1}).$$

The first subset in the right hand side satisfies

$$\sigma\left(\left(\{1,\dots,N\}\setminus E_1\right)\cap E_{k+1}\right)=\widetilde{\sigma}\left(\left(\{1,\dots,N\}\setminus E_1\right)\cap E_{k+1}\right)\subset E_k,$$

so that $\#\left(\left(\{1,\dots,N\}\setminus E_1\right)\cap E_{k+1}\right)\leq \#E_k =: m_k$.

On the other hand, $(E_1\cap E_{k+1})\subset E_1$, hence $\#(E_1\cap E_{k+1})\leq m_1$. As a consequence, $m_{k+1}\leq m_k+m_1$. This implies $m_k\leq km_1$.

As for G_k, we have:

$$G_k=(G_{k+1}\cap G_k)\cup(\sigma^{-k}(E_1)\cap G_k). \tag{17}$$

Indeed, let $n\in G_k$, i.e, $\sigma^k(n)=\widetilde{\sigma}^k(n)$. If $\sigma^{k+1}(n)=\widetilde{\sigma}^{k+1}(n)$, then $n\in G_{k+1}$. Otherwise, $\sigma^{k+1}(n)\neq\widetilde{\sigma}^{k+1}(n)$, meaning that $\sigma^{k+1}(n)\neq\widetilde{\sigma}(\sigma^k(n))$ which implies $\sigma^k(n)=\widetilde{\sigma}^k(n)\in E_1$, so that $n\in\sigma^{-k}(E_1)$. This proves (17), and we get as a by-product

$$(G_{k+1}\cap G_k)\cap(\sigma^{-k}(E_1)\cap G_k)=\emptyset.$$

Moreover, since $G_{k+1}\subset G_k$, we get $G_{k+1}\cap G_k=G_{k+1}$. It follows that

$$\#G_k=\#G_{k+1}+\#\{\sigma^{-k}(E_1)\cap G_k\}.$$

Since $\#\{\sigma^{-k}(E_1)\cap G_k\}\leq\#E_1=m_1$, we obtain $\#G_{k+1}\geq\#G_k-m_1$. The result follows. □

In what follows, a transposition in $\mathfrak{S}_N$ between two elements $i\neq j$ is denoted by $(i\ j)$. By abuse of notation, $(n\ n)$ denotes the identity for all $n=1,\dots,N$. Given a permutation $\sigma\in\mathfrak{S}_N$, we consider the sequence of permutations $(\sigma_n)_{n=0,\dots,N}$ defined by

$$\begin{aligned}&\sigma_0=\sigma\\&\sigma_n=(n\ \sigma_{n-1}(n))\circ\sigma_{n-1}.\end{aligned} \tag{18}$$

For all $n\leq N$, it immediately follows from this definition that

$$\sigma_n|_{\{1,\dots,n\}}=Id|_{\{1,\dots,n\}}\text{ and }\sigma_{N-1}=\sigma_N=Id,$$

where Id denote the identity permutation. Let us give two additional properties of this sequence.

Lemma 3. *Let $\sigma\in\mathfrak{S}_N$ and $(\sigma_n)_{n=1,\dots,N-1}$ defined by* (18)*. One has:*

$$\{i=1,\dots,N\mid\sigma(i)=i\}=\{i=1,\dots,N\mid\forall n=1,\dots,N-1,\ \sigma_n(i)=i\}.$$

Proof. Given i with $1\leq i\leq N$, such that $\sigma(i)=i$, let us prove that $\sigma_n(i)=i$ by induction on n. Since $\sigma_0=\sigma$, the result holds for $n=0$. Suppose it holds at a rank $n-1$, meaning that $\sigma_{n-1}(i)=i$. By definition of $(\sigma_n)_{n=1,\dots,N}$, one has:

$$\sigma_n(i)=(n\ \sigma_{n-1}(n))\circ\sigma_{n-1}(i)=(n\ \sigma_{n-1}(n))(i).$$

If $i=n$, then $(n\ \sigma_{n-1}(n))(i)=\sigma_{n-1}(n)=\sigma_{n-1}(i)=i$. If $i=\sigma_{n-1}(n)$, then $i=\sigma_{n-1}(i)=\sigma_{n-1}(n)$ and $i=n$, so that we conclude as in the previous case. In the other cases, $\sigma_n(i)=\sigma_{n-1}(i)=i$. The result follows. □

Lemma 4. *Let $i, j \in \{1, \dots, N\}$, with $i < j$. Let $\sigma \in \mathfrak{S}_N$ $\sigma = (i\ j) \circ \sigma'$, where $(i\ j)$ and σ' have disjoint supports, i.e., $\sigma'(i) = i$ and $\sigma'(j) = j$. One has: $\sigma_j = \sigma_{j-1}$.*

Proof. From the definition of $(\sigma_n)_{n=1,\dots,N}$, one has

$$\sigma_j = (j\ \sigma_{j-1}(j)) \circ \sigma_{j-1}.$$

We need to prove that $\sigma_{j-1}(j) = j$. Since σ' and $(i\ j)$ are disjoint, then for $n < i$, $\sigma_n = (i\ j) \circ \sigma'_n$, where σ'_n is defined by (18), with the initial term $\sigma'_0 = \sigma'$. In particular, $\sigma_n(i) = j$ for $n < i$.

In the case $n = i$, one has

$$\sigma_i = (i\ \sigma_{i-1}(i)) \circ \sigma_{i-1} = (i\ j) \circ \sigma_{i-1} = (i\ j) \circ (i\ j) \circ \sigma'_{i-1} = \sigma'_{i-1}.$$

In particular, $\sigma_i(j) = j$.

Finally, since $\sigma'_{i-1}(i) = i$, we find that $\sigma'_i = \sigma'_{i-1}$, and it follows by induction that for $n > i$, $\sigma_n = \sigma'_n$, which means $\sigma_n(j) = j$. In particular $\sigma_{j-1}(j) = j$. This concludes the proof. □

The sequence $(\sigma_n)_{n=0,\dots,N}$ can be used to decompose $J(\mathcal{I}_N) - J(P)$ for an arbitrary $P \in \mathcal{P}_N$, as stated in the next Lemma.

Lemma 5. *Let $\sigma \in \mathfrak{S}_N$ and $P \in \mathcal{P}_N$ the associated permutation matrix, we have:*

$$\langle u, (\mathcal{I}_N - P)v \rangle = \sum_{n=1}^{N-1} (u_n - u_{\sigma_{n-1}^{-1}(n)})(v_n - v_{\sigma_{n-1}(n)}).$$

Proof. Given $j \in \{0, \dots, N\}$, define $S_j = \sum_{n=1}^{N} u_n v_{\sigma_j(n)}$. Since $\sigma_j(n)$ and $\sigma_{j-1}(n)$ might only differ for $n = j$ and $n = \sigma_{j-1}^{-1}(j)$, we have

$$\begin{aligned}
S_j - S_{j-1} &= \sum_{n=j}^{N} u_n (v_{\sigma_j(n)} - v_{\sigma_{j-1}(n)}) \\
&= u_j (v_{\sigma_j(j)} - v_{\sigma_{j-1}(j)}) + u_{\sigma_{j-1}^{-1}(j)} (v_{\sigma_j(\sigma_{j-1}^{-1}(j))} - v_{\sigma_{j-1}(\sigma_{j-1}^{-1}(j))}) \\
&= u_j (v_j - v_{\sigma_{j-1}(j)}) + u_{\sigma_{j-1}^{-1}(j)} (v_{\sigma_{j-1}(j)} - v_j) \\
&= (u_j - u_{\sigma_{j-1}^{-1}(j)})(v_j - v_{\sigma_{j-1}(j)}).
\end{aligned}$$

The result then follows from $\langle u, (\mathcal{I}_N - P)v \rangle = S_{N-1} - S_0$. □

3.3 Solutions of the optimization problems

The previous lemma enables us to solve the problems $\max_{P \in \mathcal{P}_N} J^{\text{approx}}(P)$ and $\min_{P \in \mathcal{P}_N} J^{\text{approx}}(P)$. Recall that the entries of u are sorted in an ascending order.

Lemma 6. *Let $\sigma_+,\ \sigma_- \in \mathfrak{S}_N$ such that $v_{\sigma_+(1)} \leq v_{\sigma_+(2)} \cdots \leq v_{\sigma_+(N)}$ and $v_{\sigma_-(N)} \leq v_{\sigma_-(N-1)} \leq \cdots \leq v_{\sigma_-(1)}$ and $P_+,\ P_- \in \mathcal{P}_N$, the corresponding permutation matrices. Then*

$$P_+ = \mathrm{argmax}_{P\in\mathcal{P}_N} J^{approx}(P), \quad P_- = \mathrm{argmin}_{P\in\mathcal{P}_N} J^{approx}(P).$$

Proof. Let $P \in \mathcal{P}_N$ and $\sigma \in \mathfrak{S}_N$ the associated permutation, we have

$$\begin{aligned}\langle u, (P_+ - P)v\rangle =& \langle u, (\mathcal{I}_N - PP_+^{-1})w\rangle \\ =& \sum_{n=1}^{N-1} (u_n - u_{(\sigma'^{-1}_{n-1})^{-1}(n)})(w_n - w_{\sigma'_{n-1}(n)}),\end{aligned} \tag{19}$$

where $w = (w_n)_{n=1}^N := (v_{\sigma_+(n)})_{n=1}^N$ and σ'_n is the sequence defined by (18) with $\sigma' := \sigma_+^{-1} \circ \sigma$ the permutation associated with PP_+^{-1}. Since $(w_n)_{n=1}^N$ by its definition is an increasing sequence, $\sigma'_{n-1}(n) \geq n$ and $(\sigma'_{n-1})^{-1}(n) \geq n$, we find that $\langle u, (P_+ - P)v\rangle \geq 0$. The proof for the problem $\min_{P\in\mathcal{P}_N}\langle u, Pv\rangle$ is similar. □

We immediately deduce from this lemma that once u and v are given, the matrix P_+, P_- of Lemma 6 can be determined explicitly. More precisely, P_+ is the matrix corresponding to the permutation which associates the largest coefficient of u with the largest coefficient of v, the second largest coefficient with the second largest, and so on. In the same way, P_- is the matrix corresponding to the permutation which associates the largest coefficient of u with the smallest coefficient of v, the second largest coefficient with the second smallest, and so on.

Remark 2. *The optimal matrices P_+ and P_- are not unique as soon as either u or v contains at least two identical entries.*

We focus now on the case where u as well as v have entries with a constant sign. Since the results in this section hold both for minimization and maximization problems, we can assume without loss of generality that u, v are both positive. Using the properties given in the previous section, we will show that in some cases, the problem $\max_{P\in\mathcal{P}_N} J(P)$ (resp. $\min_{P\in\mathcal{P}_N} J(P)$) and $\max_{P\in\mathcal{P}_N} J^{\mathrm{approx}}(P)$ (resp. $\min_{P\in\mathcal{P}_N} J^{\mathrm{approx}}(P)$) have the same solution.

We keep the notation of Lemma 6. Define for $n = 1, \ldots, N$,

$$\widetilde{p}_n := \min_{i,j=1,\ldots,N, i\neq n, j\neq n} |(u_n - u_i)(v_{\sigma_+(n)} - v_{\sigma_+(j)})|. \tag{20}$$

Denote by i_n and j_n the solutions of the previous problem. Since $u_n, v_{\sigma_+(n)}$ are sorted in an ascending order, we find immediately that if $n = 1$ (resp. N), then $i_n = j_n = 2$ (resp. $i_n = j_n = N - 1$). Otherwise, $i_n = n - 1$ or $i_n = n + 1$, and the same result holds for j_n. Sort $(\widetilde{p}_n)_{n=1}^N$ and denote by $(p_n)_{n=1}^N$ the resulting sequence, i.e., $p_1 \leq, \ldots, \leq p_N$. Define then for $m = 1, \ldots, N$

$$s_m := \sum_{n=1}^{m} p_n, \tag{21}$$

and

$$F_m^- := \sum_{n=1}^{\min(m,N)} u_n v_{\sigma_-(N-m+n)}, \quad F_m^+ := \sum_{n=\max(1,N-m+1)}^{N} u_n v_{\sigma_+(n)}. \tag{22}$$

From the definition of these sequences, we have $F_m^+ \geq F_m^-$. See Appendix C for the case where u or v negative. We are now in a position to give the main result of this section.

Theorem 1. *Assume that u and v have positive entries and define*

$$\phi(m_1) := \frac{1}{s_{\lceil \frac{m_1}{2} \rceil}} \Big(\sum_{l=1}^{+\infty} d_{\max}^l F_{(l+1)m_1}^+ - d_{\min}^l F_{(l+1)m_1}^- \Big), \tag{23}$$

where m_1 refers to the notation in Lemma 2, $d_{\max} := \max_{n=1,\ldots,N}(d_n)$ and $d_{\min} := \min_{n=1,\ldots,N}(d_n)$. Assume that:

$$\max_{m_1 \geq 2} \phi(m_1) \leq 1. \tag{24}$$

Then the problem $\max_{P \in \mathcal{P}_N} \langle u, (\mathcal{I}_N - PD)^{-1} Pv \rangle$ (resp. $\min_{P \in \mathcal{P}_N} \langle u, (\mathcal{I}_N - PD)^{-1} Pv \rangle$) and the problem $\max_{P \in \mathcal{P}_N} \langle u, Pv \rangle$ (resp. $\min_{P \in \mathcal{P}_N} \langle u, Pv \rangle$) have the same solution.

Proof. We keep the notation in Section 3.2 and give the proof in the case of the maximization problem. The case of the minimization problem can be handled in much the same way. Let $P \in \mathcal{P}_N$ and $\sigma \in \mathfrak{S}_N$ the associated permutation, we have

$$\begin{aligned} & \langle u, (\mathcal{I}_N - P_+ D)^{-1} P_+ v \rangle - \langle u, (\mathcal{I}_N - PD)^{-1} Pv \rangle & (25) \\ = & \sum_{l=0}^{+\infty} \langle u, \big((P_+ D)^l P_+ - (PD)^l P \big) v \rangle \\ = & \langle u, (P_+ - P) v \rangle + \sum_{l=1}^{+\infty} \langle u, \big((P_+ D)^l P_+ - (PD)^l P \big) v \rangle. & (26) \end{aligned}$$

From the definition $E_k(\sigma_+, \sigma)$ and $G_k(\sigma_+, \sigma)$, we have $E_1(\sigma_+, \sigma) \sqcup G_1(\sigma_+, \sigma) = \{1, \ldots, N\}$. Let us denote by $(w_n)_{n=1}^N = (v_{\sigma_+(n)})_{n=1}^N$ and by σ'_n the sequence defined by (18) with $\sigma'_0 := \sigma_+^{-1} \circ \sigma$. From the definition of $E_1(\sigma_+, \sigma)$ and $G_1(\sigma_+, \sigma)$, we have $\sigma(G_1(\sigma_+, \sigma)) = \sigma_+(G_1(\sigma_+, \sigma))$ and $\sigma(E_1(\sigma_+, \sigma)) = \sigma_+(E_1(\sigma_+, \sigma))$, which implies $\sigma'_0(E_1(\sigma_+, \sigma)) = E_1(\sigma_+, \sigma)$, and for any $i \in G_1(\sigma_+, \sigma)$, $\sigma'_0(i) = i$.

Using these properties and (19), we have

$$\begin{aligned}\langle u,(P_+-P)v\rangle &= \sum_{n=1}^{N-1}(u_n-u_{(\sigma'_{n-1})^{-1}(n)})(w_n-w_{\sigma'_{n-1}(n)})\\ &= \sum_{n\in E_1(\sigma_+,\sigma)}(u_n-u_{(\sigma'_{n-1})^{-1}(n)})(w_n-w_{\sigma'_{n-1}(n)})\\ &\quad+\sum_{n\in G_1(\sigma_+,\sigma)}(u_n-u_{(\sigma'_{n-1})^{-1}(n)})(w_n-w_{\sigma'_{n-1}(n)})\\ &= \sum_{n\in E_1(\sigma_+,\sigma)}(u_n-u_{(\sigma'_{n-1})^{-1}(n)})(w_n-w_{\sigma'_{n-1}(n)}).\end{aligned} \tag{27}$$

In the case where there exists a transposition $(i\ i')$ with $i<i'$ in σ', Lemma 4 implies that $u_{(\sigma'_{i'-1})^{-1}(i')}=u_{i'}$ and $w_{\sigma'_{i'-1}(i')}=w_{i'}$. The maximum number of transpositions in σ'_0 is $\frac{m_1}{2}$ if m_1 is even, $\frac{m_1-3}{2}$ otherwise. Hence, the smallest number of non-zero terms present in the last sum of (27) is given by $m_1-\frac{m_1}{2}=\frac{m_1}{2}$ if m_1 is even, $\frac{m_1-1}{2}$ otherwise. In other words, there exists at least $\lceil\frac{m_1}{2}\rceil$ non zero terms in the last sum of (27), which implies

$$\langle u,(P_+-P)v\rangle = \sum_{n\in E_1(\sigma_+,\sigma)}(u_n-u_{(\sigma'_{n-1})^{-1}(n)})(w_n-w_{\sigma'_{n-1}(n)})\geq s_{\lceil\frac{m_1}{2}\rceil}. \tag{28}$$

For $n\in\{1,\dots,N\}$ and $l\in\mathbb{N}^*$, let us denote by $d_{\sigma,l,n}:=d_{\sigma^l(n)}d_{\sigma^{l-1}(n)}\cdots d_{\sigma(n)}$. Considering now the second term of the right hand side of (26), we get

$$<u,(PD)^lPv>=\sum_{n=1}^{N}u_nd_{\sigma^l(n)}d_{\sigma^{l-1}(n)}\cdots d_{\sigma(n)}v_{\sigma^{l+1}(n)}=\sum_{n=1}^{N}u_nd_{\sigma,l,n}v_{\sigma^{l+1}(n)}.$$

Using this notation and Lemma 2, we find

$$\begin{aligned}&\left|\langle u,(P_+D)^lP_+v-(PD)^lPv\rangle\right|\\ =&\left|\sum_{n=1}^{N}u_n(d_{\sigma_+,l,n}v_{\sigma_+^{l+1}(n)}-d_{\sigma,l,n}v_{\sigma^{l+1}(n)})\right|\\ =&\left|\sum_{n\notin G_{l+1}(\sigma_+,\sigma)}u_n(d_{\sigma_+,l,n}v_{\sigma_+^{l+1}(n)}-d_{\sigma,l,n}v_{\sigma^{l+1}(n)})\right|\\ =&\left|\sum_{n\notin G_{l+1}(\sigma_+,\sigma)}u_nd_{\sigma_+,l,n}v_{\sigma_+^{l+1}(n)}-\sum_{n\notin G_{l+1}(\sigma_+,\sigma)}u_nd_{\sigma,l,n}v_{\sigma^{l+1}(n)}\right|\\ \leq&d_{\max}^l\sum_{n\notin G_{l+1}(\sigma_+,\sigma)}u_nv_{\sigma_+(n)}-d_{\min}^l\sum_{n\notin G_{l+1}(\sigma_+,\sigma)}u_nv_{\sigma_-(n)}\\ \leq&d_{\max}^lF^+_{(l+1)m_1}-d_{\min}^lF^-_{(l+1)m_1}.\end{aligned} \tag{29}$$

This result combined with (24), gives

$$\left|\sum_{l=1}^{+\infty}\langle u,(P_+D)^lP_+v-(PD)^lPv\rangle\right| \leq \sum_{l=1}^{+\infty} d_{\max}^l F^+_{(l+1)m_1} - d_{\min}^l F^-_{(l+1)m_1}$$
$$\leq s_{\lceil \frac{m_1}{2}\rceil}.$$

Considering now (28), we obtain

$$|\langle u,(P_+-P)v\rangle| \geq \left|\sum_{l=1}^{+\infty}\langle u,(P_+D)^lP_+v-(PD)^lPv\rangle\right|.$$

It follows that the first term of (26) dominates the second one. As a consequence, the former has the same sign as (25). The result follows. □

3.4 Implementation remarks

Let us conclude with some remarks on the computation of the function $\phi(m_1)$, more precisely of the sum in (23). Given $m_1 \in \{2,\dots,N\}$, define by l^* such that

$$l^* := \left\lfloor \frac{N}{m_1} \right\rfloor - 1.$$

We have

$$\begin{aligned}
&\sum_{l=1}^{+\infty} \left(d_{\max}^l F^+_{(l+1)m_1} - d_{\min}^l F^-_{(l+1)m_1}\right)\\
=&\sum_{l=1}^{l^*} \left(d_{\max}^l F^+_{(l+1)m_1} - d_{\min}^l F^-_{(l+1)m_1}\right) + \sum_{l=l^*+1}^{+\infty} \left(d_{\max}^l F^+_{(l+1)m_1} - d_{\min}^l F^-_{(l+1)m_1}\right)\\
=&\sum_{l=1}^{l^*} \left(d_{\max}^l F^+_{(l+1)m_1} - d_{\min}^l F^-_{(l+1)m_1}\right) + \frac{d_{\max}^{l^*+1}}{1-d_{\max}} F_N^+ - \frac{d_{\min}^{l^*+1}}{1-d_{\min}} F_N^-.
\end{aligned}$$

As for the evaluation of $s_{\lceil \frac{m_1}{2}\rceil}$, only $\lceil \frac{N}{2}\rceil$ terms need to be computed. Examples of behaviour of s_m and F_m^+, F_m^- are presented in Figure 3, whereas examples of behaviour of the function (23) with respect to m_1 are shown in Figure 4.

4 Numerical experiments

In this section, we present some numerical results to evaluate the efficiency of the mixing strategies and their approximation.

4.1 Parameter settings

Consider a raceway whose water elevation $h = 0.4\,\mathrm{m}$, which corresponds to typical raceway pond setting. All the numerical parameters values considered in this section for Han's model are taken from [16] and recalled in Table 1. Recall that I_s is the light intensity at the free surface. In order to fix the value

Table 1: Parameter values for Han Model

k_r	$6.8\ 10^{-3}$	s^{-1}
k_d	$2.99\ 10^{-4}$	-
τ	0.25	s
σ_H	0.047	$\mu\mathrm{mol}\cdot\mathrm{m}^{-2}\,\mathrm{s}^{-1}$
k_H	$8.7\ 10^{-6}$	-
R	$1.389\ 10^{-7}$	s^{-1}

of the light extinction coefficient ε in (3), we assume that only a fraction q of I_s reaches the bottom of the raceway pond, meaning that $I_b = qI_s$, where $q \in [0, 1]$ and I_b is the light intensity at the bottom. It follows that ε can be computed by

$$\varepsilon = (1/h)\ln(1/q).$$

In practice, this quantity can be implemented in the experiments by adapting the biomass harvesting frequency, or the dilution rate for continuous cultivation. In what follows, the varying parameters are I_s , the ratio q and T. We consider $I_s \in [0, 2500]\mu\mathrm{mol}\,\mathrm{m}^{-2}\,\mathrm{s}^{-1}$, $q \in [0.1\%, 10\%]$ and $T \in [1, 1000]$s. The number of layers N remains small as we need to test numerically $N!$ permutation matrices for each triplet (I_s, q, T).

4.2 Numerical tests

As shown in [6, Section IV.B], Problem (12) admits non trivial optimal permutation strategies which may significantly change according to the parameter settings. In this section, we study and compare the true and the approximated solutions as well as their efficiency with respect to the average net specific (4).

We start by investigating some properties of the items defined in the previous sections. Recall that the two sequences u, v used in Section 3 correspond in our application to Γ, V respectively. We consider $N = 20$ layers and two parameters triplets, namely $(I_s, q, T) = (2000, 5\%, 1000)$ and (800,0.5%,1). Figure 2 shows the evolution of these two quantities as a function of I. Note that in both cases, V is positive with sorted entries, as can be seen in (8). On the contrary, the discretized Γ is negative and not necessarily sorted. We refer to Appendix A for more details about V and Γ.

We then study the behaviour of the sequences F_m^+, F_m^-, s_m and $\phi(m_1)$ defined in Section 3.3 for the same two parameters triplets. Note that since Γ is negative,

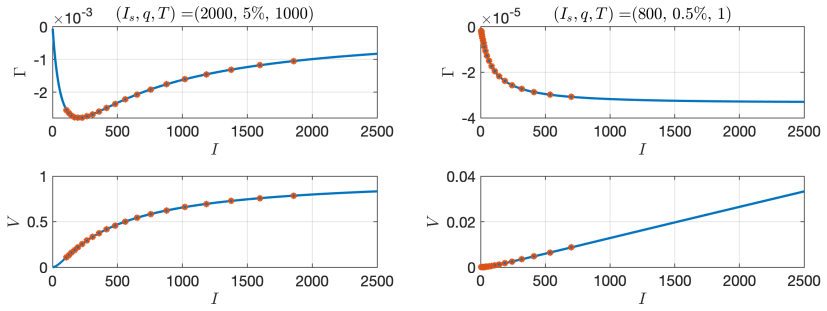

Figure 2: Γ and V with respect to the light intensity I (Blue curve). Discretisation points (Red point) chosen for $(I_s, q, T) = (2000, 5\%, 1000)$ (Left) and (800,0.5%,1) (Right).

F_m^- and F_m^+ are defined as in Appendix C (and not as in (22)). We choose $N = 7$ and $N = 20$ to check the performance for two different discretisation numbers of layers. One can see in Figure 4 that the maximal value of $\phi(m_1)$ is always obtained for $m_1 = 2$, and that the maximal value $\phi(m_1)$ appears to be an increasing function of N. This makes the criterion given in Section 3.3 less efficient for a large number of layers N. Further analysis is required to obtain a criterion that does not depend on N.

The next test is devoted to the convergence of the average growth rate $\bar{\mu}_N$ with respect to the number of layers N. We keep the two triplets of parameters of the previous test. Due to the limit of the computer memory, the computation of $\bar{\mu}_N(P_{\max})$ is tractable for small values of N, in our case lower than or equal to $N = 11$. Such an issue does not occur in the case of $\bar{\mu}_N(P_+)$. Figure 5 presents the behaviour of $\bar{\mu}_N$. For the parameter triplet (2000,5%,1000), the criterion is satisfied until $N = 7$ (green circle), which is confirmed in Figure 4 (Left) where the maximal value of $\phi(m_1)$ is already close to 1. Though the criterion is not satisfied for $N > 7$, we observe that $P_+ = P_{\max}$ from $N = 2$ to $N = 11$. As for the triplet (800,0.5%,1), one can see that $P_+ = P_{\max}$ until $N = 3$. Figure 6 shows the optimal matrices for these two different parameter triplets in the case $N = 11$ and $N = 100$. It can be observed that for the parameter triplet (2000,5%,1000), the two matrices $P_+, P_{\max}$ have the same form for $N = 11$ and $N = 100$ (Figure 6 Top). Hence, one can expect $P_{\max} = P_+$ for larger N. However, this may not be the case for (800,0.5%,1) since $P_+, P_{\max}$ have already different forms for $N = 11$ (Figure 6 Bottom).

In the following tests, we focus only on two special cases: large lap duration time ($T = 1000\,\mathrm{s}$) and small lap duration time ($T = 1\,\mathrm{s}$). In practise, the former corresponds to typical time required to complete one lap in a raceway pond system, whereas the latter rather corresponds to photobioreactor [21]. In the small lap duration time case, we observe the so-called *flashing effect*. This phenomenon corresponds to the fact that the growth rate is an increasing function of the the light exposition frequency. It can be observed in Figure 7,

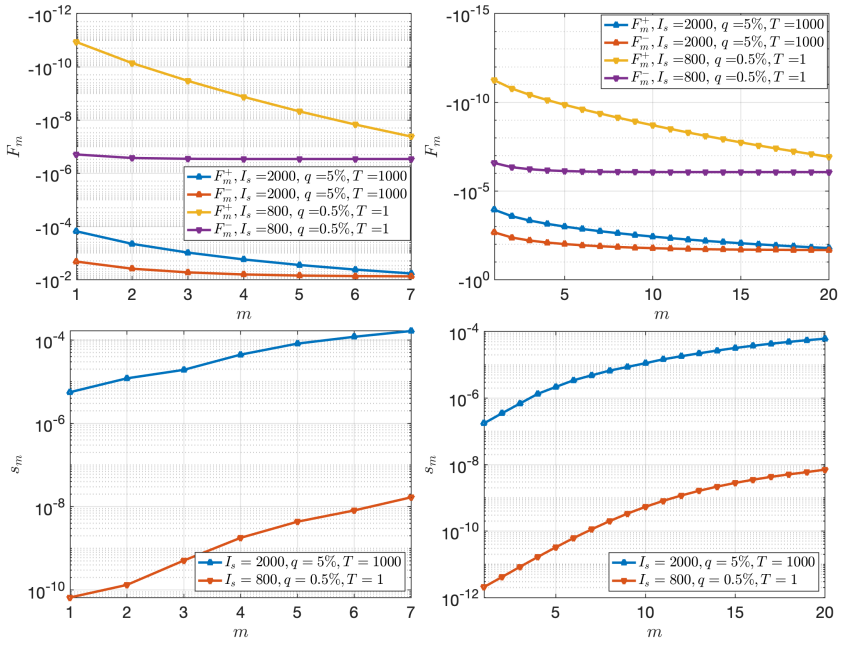

Figure 3: Example of sequences F_m^+, F_m^- (Top) and s_m (Bottom) with respect to m for the two parameters triplets. Left: $N = 7$. Right: $N = 20$.

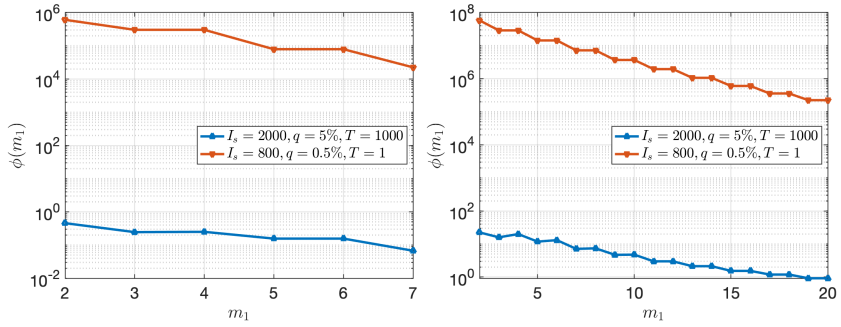

Figure 4: Example of behaviour of $\phi(m_1)$ with respect to m_1 for two parameters triplets and two different N. Left: $N = 7$. Right: $N = 20$.

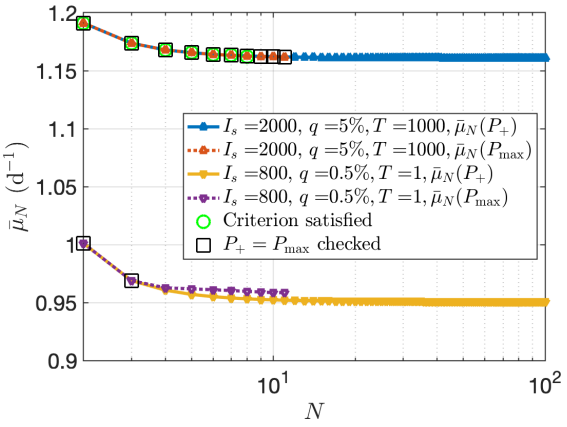

Figure 5: Average growth rate $\bar{\mu}_N$ obtained with $P_{\max}$ and P_+ as a function of N for the two parameters triplets. The green circles mark the case when the criterion is satisfied. The black squares mark the case when $P_{\max} = P_+$ is observed.

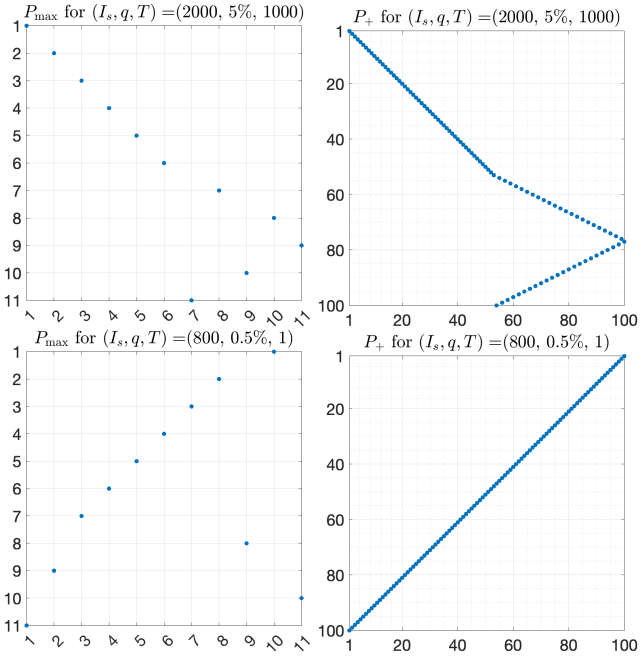

Figure 6: Optimal matrix $P_{\max}$ for Problem (12) and $N = 11$ (Left) and P_+ for Problem (14) and $N = 100$ (Right) for the two parameters triplets. The blue points represent non-zero entries, i.e., entries equal to 1.

where $\bar{\mu}_N(P_{\max})$ decreases with respect to T for all considered light intensities. This phenomenon has already been reported in literature, see, e.g. [21].

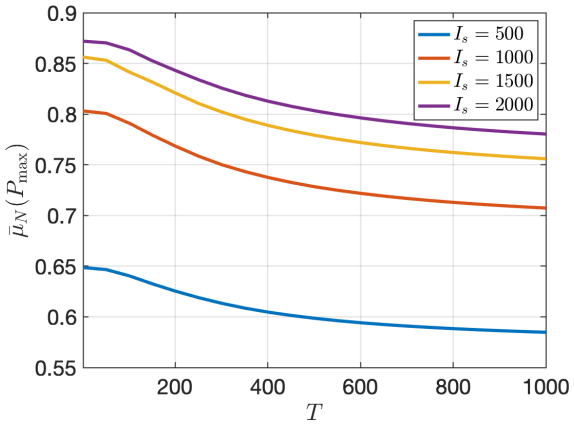

Figure 7: Average specific growth rate in the case $q = 0.1\%$ and $N = 7$ for four different light intensities I_s.

The next test is dedicated to the efficiency of the criterion (24). More precisely, we evaluate the value of the function $\bar{\mu}_N$ defined by (10) for the optimal matrix $P_{\max}$ which solves Problem (12) and for the matrix P_+ which solves the approximated Problem (13). We consider two different discretisation values $N = 5$ and $N = 9$. Figure 8 shows the results for $T = 1\,\mathrm{s}$ and $T = 1000\,\mathrm{s}$. We see that for large values of T, the optimum approximation almost always coincides to the true optimum. Nevertheless, we observe that the criterion (24) becomes less efficient for larger N. Note that the case corresponding to $I_s = 0\,\mu\mathrm{mol\,m^{-2}\,s^{-1}}$ is particular since no light is available in the system, implying that Γ, V equal to zero. In this case the value of the functionals do not depend on P. Hence $\bar{\mu}_N(P_{\max}) = \bar{\mu}_N(P_+)$ when $I_s = 0\,\mu\mathrm{mol\,m^{-2}\,s^{-1}}$.

We finally evaluate the efficiency of various mixing strategies. Define

$$r_1 := \frac{\bar{\mu}_N(P_{\max}) - \bar{\mu}_N(\mathcal{I}_N)}{\bar{\mu}_N(\mathcal{I}_N)}, \tag{30}$$

$$r_2 := \frac{\bar{\mu}_N(P_{\max}) - \bar{\mu}_N(P_{\min})}{\bar{\mu}_N(P_{\min})}, \tag{31}$$

$$r_3 := \frac{\bar{\mu}_N(\mathcal{I}_N) - \bar{\mu}_N(P_{\min})}{\bar{\mu}_N(\mathcal{I}_N)}, \tag{32}$$

where $P_{\min} \in \mathcal{P}_N$ is the matrix that minimizes J, (see (11)), i.e., that corresponds to the worse strategy. We consider $N = 9$ layers. Figure 9 presents the results for $T = 1\,\mathrm{s}$ and $T = 1000\,\mathrm{s}$. Better performance is in most cases obtained for a small time duration $T = 1\,\mathrm{s}$. In this way, we observe that the relative improvement between the best and the no mixing strategy may reach 15%, whereas the relative improvement between the worst and the best strategy

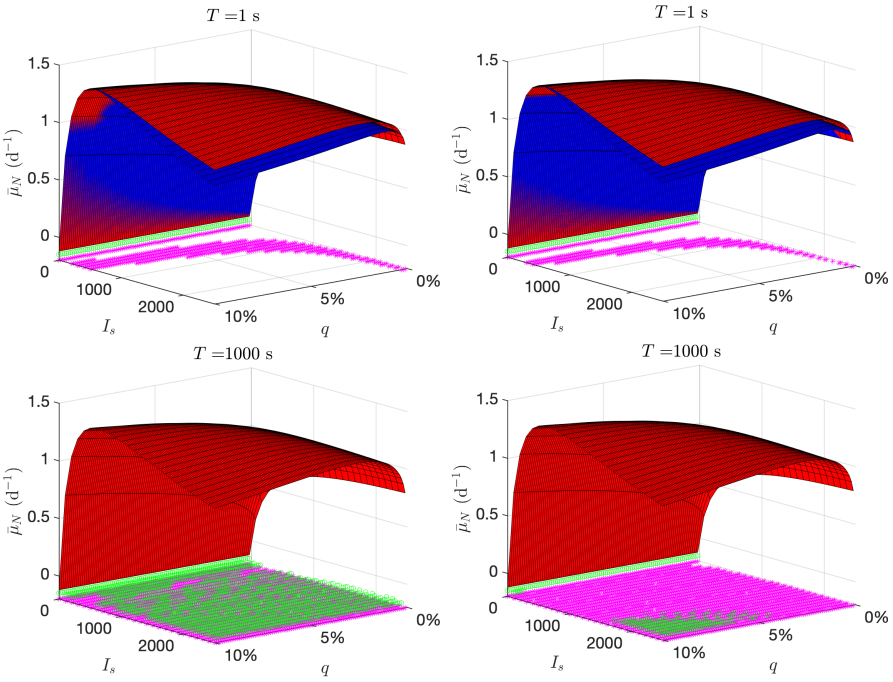

Figure 8: Average net specific growth rate $\bar{\mu}_N$ for $T = 1\,\mathrm{s}$ (Top) and for $T = 1000\,\mathrm{s}$ (Bottom). Left: $N = 5$. Right: $N = 9$. The red surface is obtained with $P_{\max}$ and the blue surface is obtained with P_+. The purple stars represent the cases where $P_{\max} = P_+$ or, in case of multiple solution, $\bar{\mu}_N(P_{\max}) = \bar{\mu}_N(P_+)$. The green circle represent the cases where the criterion (24) is satisfied.

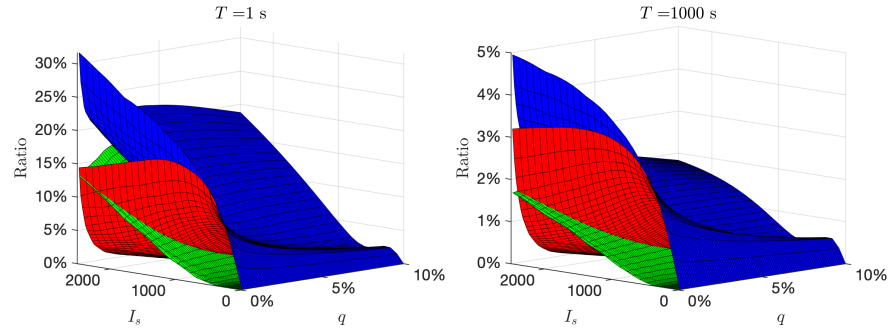

Figure 9: Three ratios (30)- (32) for $T = 1\,\mathrm{s}$ (Left) and for $T = 1000\,\mathrm{s}$ (Right). In each figure, the red surface represents r_1, the blue surface represents r_2 and the green surface represents r_3.

may reach 30%. In both two cases, a better improvement can be obtained with high values of I_s and low values of q.

To compare the efficiency of the approximation P_+ with respect the true optimal mixing strategy $P_{\max}$, we define two extra ratios:

$$\tilde{r}_1 := \frac{\bar{\mu}_N(P_+) - \bar{\mu}_N(\mathcal{I}_N)}{\bar{\mu}_N(\mathcal{I}_N)}, \tag{33}$$

$$\tilde{r}_2 := \frac{\bar{\mu}_N(P_+) - \bar{\mu}_N(P_{\min})}{\bar{\mu}_N(P_{\min})}. \tag{34}$$

Figure 10 presents the results for $T = 1\,\mathrm{s}$ and $T = 1000\,\mathrm{s}$. As already mentioned,

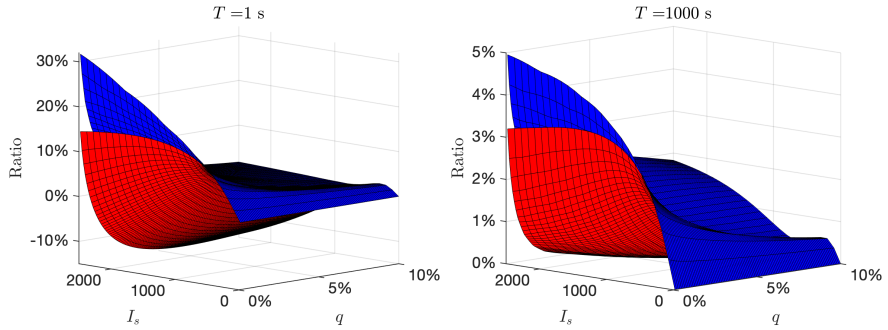

Figure 10: Two ratios (33)- (34) for $T = 1\,\mathrm{s}$ (Left) and for $T = 1000\,\mathrm{s}$ (Right). In each figure, the red surface represents $\tilde{r}_1$, the blue surface represents $\tilde{r}_2$.

for a large lap duration time, the optimization problem (14) provides a good approximation.

This can be observed with the blue and red surface in Figure 9 (Right) and in Figure 10 (Right), both surfaces have the same behaviours. As expected, the approximation becomes less efficient in the case of short lap duration time. This can be observed in Figure 9 (Left) and in Figure 10 (Left). However, the maximal values of r_1, r_2 are still preserved by their approximations $\tilde{r}_1, \tilde{r}_2$.

5 Conclusion

We have presented a model of raceway that focuses on the mixing generated by the flow driving device. This model enables us to find mixing strategies that maximize the production. Thought reducing the computation to one lap, a significant computational effort is required when dealing with fine discretisation of the fluid layers. We overcome this difficulty by defining an approximation that has an explicit solution that appears to coincide with the true solution when the lap duration T is large enough. Our experimental results show the significance of the choice of the mixing strategy: the relative ratio between the best and the worst case reaches 30% in some cases. We also observe a flashing effect meaning that better results are obtained when T goes to zero.

Further works will be devoted to the improvement of the function ϕ used in Theorem 1 in order to improve our approach for large number of layers N.

References

[1] Richmond Amos. Principles for attaining maximal microalgal productivity in photobioreactors: an overview. *Hydrobiologia*, 512(1):33–37, 2004.

[2] G. Becerra-Celis, G. Hafidi, S. Tebbani, D. Dumur, and A. Isambert. Nonlinear predictive control for continuous microalgae cultivation process in a photobioreactor. In *2008 10th International Conference on Control, Automation, Robotics and Vision*, pages 1373–1378, 2008.

[3] Olivier Bernard, Liu-Di Lu, Jacques Sainte-Marie, and Julien Salomon. Controlling the bottom topography of a microalgal pond to optimize productivity. To appear in the Proceedings of the 2021 American Control Conference (ACC 2021), October 2020.

[4] Olivier Bernard, Liu-Di Lu, Jacques Sainte Marie, and Julien Salomon. Shape optimization of a microalgal raceway to enhance productivity. Submitted paper, November 2021.

[5] Olivier Bernard, Liu-Di Lu, and Julien Salomon. Mixing strategies combined with shape design to enhance productivity of a raceway pond. To appear in the Proceedings of the 11th IFAC SYMPOSIUM on Advanced Control of Chemical Processes(ADCHEM2021), 2021.

[6] Olivier Bernard, Liu-Di Lu, and Julien Salomon. Optimizing microalgal productivity in raceway ponds through a controlled mixing device. To appear in the Proceedings of the 2021 American Control Conference (ACC 2021), October 2021.

[7] Dimitris Bertsimas and John N. Tsitsiklis. *Introduction to Linear Optimization*. Athena Scientific, 1997.

[8] R. Burkard, M. Dell'Amico, and S. Martello. *Assignment Problems*. SIAM, 2008.

[9] David Chiaramonti, Matteo Prussi, David Casini, Mario R. Tredici, Liliana Rodolfi, Niccolò Bassi, Graziella Chini Zittelli, and Paolo Bondioli. Review of energy balance in raceway ponds for microalgae cultivation: Rethinking a traditional system is possible. *Applied Energy*, 102:101 – 111, 2013. Special Issue on Advances in sustainable biofuel production and use - XIX International Symposium on Alcohol Fuels - ISAF.

[10] Jean-François Cornet. Calculation of optimal design and ideal productivities of volumetrically lightened photobioreactors using the constructal approach. *Chemical Engineering Science*, 65(2):985–998, 2010.

[11] Jean-François Cornet and Claude-Gilles Dussap. A simple and reliable formula for assessment of maximum volumetric productivities in photobioreactors. *Biotechnology Progress*, 25(2):424–435, 2009.

[12] María Cuaresma, Marcel Janssen, Evert Jan van den End, Carlos Vílchez, and René H. Wijffels. Luminostat operation: A tool to maximize microalgae photosynthetic efficiency in photobioreactors during the daily light cycle? *Bioresource Technology*, 102(17):7871–7878, 2011.

[13] H. De la Hoz Siegler, W.C. McCaffrey, R.E. Burrell, and A. Ben-Zvi. Optimization of microalgal productivity using an adaptive, non-linear model based strategy. *Bioresource Technology*, 104:537–546, 2012.

[14] David Demory, Charlotte Combe, Philipp Hartmann, Amélie Talec, Eric Pruvost, Raouf Hamouda, Fabien Souillé, Pierre-Olivier Lamare, Marie-Odile Bristeau, Jacques Sainte-Marie, Sophie Rabouille, Francis Mairet, Antoine Sciandra, and Olivier Bernard. How do microalgae perceive light in a high-rate pond? towards more realistic lagrangian experiments. *The Royal Society*, May 2018.

[15] Michel HM Eppink, Giuseppe Olivieri, Hans Reith, Corjan van den Berg, Maria J Barbosa, and Rene H Wijffels. From current algae products to future biorefinery practices: a review. In *Biorefineries*, pages 99–123. Springer, 2017.

[16] Jérôme Grenier, F. Lopes, Hubert Bonnefond, and Olivier Bernard. Worldwide perspectives of rotating algal biofilm up-scaling. Submitted paper, 2020.

[17] Frédéric Grognard, Andrei R. Akhmetzhanov, and Olivier Bernard. Optimal strategies for biomass productivity maximization in a photobioreactor using natural light. *Automatica*, 50(2):359–368, 2014.

[18] Bo-Ping Han. Photosynthesis–irradiance response at physiological level: A mechanistic model. *Journal of theoretical biology*, 213(2):121–127, November 2001.

[19] Qiang Hu, Milton Sommerfeld, Eric Jarvis, Maria Ghirardi, Matthew Posewitz, Michael Seibert, and Al Darzins. Microalgal triacylglycerols as feedstocks for biofuel production: perspectives and advances. *The Plant Journal*, 54(4):621–639, 2008.

[20] Leonid Kantorovich. On the transfer of masses (in russian). *Doklady Akademii Nauk*, 37(2):227–229, 1942.

[21] Pierre-Olivier Lamare, Nina Aguillon, Jacques Sainte-Marie, Jérôme Grenier, Hubert Bonnefond, and Olivier Bernard. Gradient-based optimization of a rotating algal biofilm process. *Automatica*, 105:80–88, 2019.

[22] EH Lieb. Variational principle for many-fermion systems. *Physical Review Letters*, 46(7):457–459, 1981.

[23] Rafael Munoz Tamayo, Francis Mairet, and Olivier Bernard. Optimizing microalgal production in raceway systems. *Biotechnology Progress*, 29(2):543–552, 2013.

[24] Stuart A Scott, Matthew P Davey, John S Dennis, Irmtraud Horst, Christopher J Howe, David J Lea-Smith, and Alison G Smith. Biodiesel from algae: challenges and prospects. *Current Opinion in Biotechnology*, 21(3):277–286, 2010. Energy biotechnology – Environmental biotechnology.

[25] Pauline Spolaore, Claire Joannis-Cassan, Elie Duran, and Arsène Isambert. Commercial applications of microalgae. *Journal of Bioscience and Bioengineering*, 101(2):87–96, 2006.

[26] René H Wijffels and Maria J Barbosa. An outlook on microalgal biofuels. *Science*, 329(5993):796–799, 2010.

A Explicit Computations

In this appendix, we provide the computational details to solve (1) and (6) for an arbitrary layer $n \in \{1, \dots, N\}$. Given two points $t_1, t_2 \in [0, T]$. Since I_n is constant, Equation (1) can be integrated and becomes

$$C_n(t_2) = e^{\alpha(I_n)(t_1-t_2)} C_n(t_1) + \frac{\beta(I_n)}{\alpha(I_n)}(1 - e^{\alpha(I_n)(t_1-t_2)}). \tag{35}$$

The time integral in (6) can be computed by

$$\int_0^T \mu(C_n(t), I_n)\mathrm{d}t = \int_0^T -\gamma(I_n)C_n(t) + \zeta(I_n)\mathrm{d}t = -\gamma(I_n)\int_0^T C_n(t)\mathrm{d}t + \zeta(I_n)T.$$

Replacing t_2 by t and t_1 by 0 in (35) and integrating t from 0 to T gives

$$\begin{aligned}\int_0^T C_n(t)\mathrm{d}t =& \int_0^T \Big(e^{-\alpha(I_n)t}C_n(0) + \frac{\beta(I_n)}{\alpha(I_n)}(1 - e^{-\alpha(I_n)t})\Big)\mathrm{d}t \\ =& \frac{C_n(0)}{\alpha(I_n)}(1 - e^{-\alpha(I_n)T}) + \frac{\beta(I_n)}{\alpha(I_n)}T - \frac{\beta(I_n)}{\alpha^2(I_n)}(1 - e^{-\alpha(I_n)T}).\end{aligned}$$

Using notations given in Section 2.3, we have

$$\Gamma = \frac{\gamma(I)}{\alpha(I)}(e^{-\alpha(I)T} - 1), \quad V = \frac{\beta(I)}{\alpha(I)}(1 - e^{-\alpha(I)T}).$$

From the definition of $\alpha(I), \beta(I), \gamma(I)$, we find

$$\begin{aligned}\frac{\beta(I)}{\alpha(I)} &= \frac{\beta(I)}{\beta(I) + k_r} = \frac{k_d\tau(\sigma_H I)^2}{k_d\tau(\sigma_H I)^2 + k_r\tau\sigma_H I + k_r}, \\ \frac{\gamma(I)}{\alpha(I)} &= \frac{k_H\sigma_H I}{k_d\tau(\sigma_H I)^2 + k_r\tau\sigma_H I + k_r}.\end{aligned}$$

Remark that Γ and V always have the opposite sign. Note also that $I \mapsto \frac{\beta(I)}{\alpha(I)}$ is increasing on $[0, +\infty)$, which is not the case for $I \mapsto \frac{\gamma(I)}{\alpha(I)}$. It follows that V increases on $\mathbb{R}^+$ and Γ is not monotonic on $\mathbb{R}^+$ (see Figure 2).

B Optimization problem with arbitrary vectors

Let $\tilde{u}, v \in \mathbb{R}^N$ two arbitrary vectors. Let $Q \in \mathcal{P}_N$ such that $u := Q\tilde{u}$ has entries sorted in an ascending order. Since Q is a permutation matrix, we have $Q^T = Q^{-1}$. For any $P \in \mathcal{P}_N$, let us denote by $\tilde{P} := Q^{-1}PQ$, we have $\tilde{P} \in \mathcal{P}_N$ a permutation matrix. Let us denote by $\tilde{v} := Q^{-1}v$ and by $\tilde{D} = Q^{-1}DQ$. Note that $\tilde{D}$ is still a diagonal matrix with a different order of the diagonal coefficients. Using this notation, we find for the objective function (15) satisfies

$$\begin{aligned} J(P) := \langle u, (\mathcal{I}_N - PD)^{-1}Pv\rangle &= \langle \tilde{u}, Q^{-1}(\mathcal{I}_N - PD)^{-1}QQ^{-1}PQQ^{-1}v\rangle \\ &= \langle \tilde{u}, \left(Q^{-1}(\mathcal{I}_N - PD)Q\right)^{-1}\tilde{P}\tilde{v}\rangle \\ &= \langle \tilde{u}, (Q^{-1}Q - Q^{-1}PQQ^{-1}DQ)^{-1}\tilde{P}\tilde{v}\rangle \\ &= \langle \tilde{u}, (\mathcal{I}_N - \tilde{P}\tilde{D})^{-1}\tilde{P}\tilde{v}\rangle. \end{aligned}$$

For the objective function (16), we get

$$J^{\text{approx}}(P) := \langle u, Pv\rangle = \langle \tilde{u}, Q^{-1}PQQ^{-1}v\rangle = \langle \tilde{u}, \tilde{P}\tilde{v}\rangle.$$

Therefore, these problems can still be treated similarly in the general case.

C Remark on F_m^+, F_m^-

Let $u, v \in \mathbb{R}^N$ such that the entries of u are sorted in an ascending order. One should be careful when defining the two sequences F_m^+ and F_m^- in Section 3.3, since the sign of u and v plays an important role in the definition of these two sequences. For instance, assume that u is now negative and v is positive. Let $\tilde{u} := -u$, since u is assumed to be sorted in an ascending order, $\tilde{u}$ is positive and sorted in a descending order. Using the definition in (22), one has

$$\tilde{F}_m^+ := \sum_{n=1}^{\min(m,N)} \tilde{u}_n v_{\tilde{\sigma}_+(n)}, \quad \tilde{F}_m^- := \sum_{n=\max(1,N-m+1)}^{N} \tilde{u}_n v_{\tilde{\sigma}_-(2N-m-n+1)},$$

where $v_{\tilde{\sigma}_+(1)} \geq v_{\tilde{\sigma}_+(2)} \geq, \ldots, \geq v_{\tilde{\sigma}_+(N)}$ and $v_{\tilde{\sigma}_-(1)} \leq v_{\tilde{\sigma}_-(2)} \leq, \ldots, \leq v_{\tilde{\sigma}_-(N)}$. Let us define by $\sigma_+ := \tilde{\sigma}_-$ and $\sigma_- := \tilde{\sigma}_+$. One has

$$\tilde{F}_m^+ = -\sum_{n=1}^{\min(m,N)} u_n v_{\sigma_-(n)}, \quad \tilde{F}_m^- = -\sum_{n=\max(1,N-m+1)}^{N} u_n v_{\sigma_+(2N-m-n+1)}.$$

Therefore, in this case we can define F_m^+ and F_m^- by

$$F_m^- := \sum_{n=1}^{\min(m,N)} u_n v_{\sigma_-(n)}, \quad F_m^+ := \sum_{n=\max(1,N-m+1)}^{N} u_n v_{\sigma_+(2N-m-n+1)}.$$

The case where u is positive and v is negative, or both u, v are negative can be treated in a similar way.